Cellulose (2012) 19:2093–2104
DOI 10.1007/s10570-012-9775-4

ORIGINAL PAPER

Structural characterisation of thiol-modified hyaluronans

Eva Hrabárová · Jozef Rychlý · Vlasta Sasinková · Katarína Valachová · Ivica Janigová · Katarína Csomorová · Ivo Juránek · Ladislav Šoltés

Received: 15 May 2012 / Accepted: 25 August 2012 / Published online: 12 September 2012

Abstract Fourier-transform infrared spectroscopy and non-isothermal methods—chemiluminometry, differential scanning calorimetry, and differential thermogravimetry—were used to characterize potential structural changes of thiol-modified hyaluronans. Degradative conditions tested via rotational viscometry were first initiated applying oxidative *Weissberger*'s system in a reaction system under aerobic conditions. Several low-molecular-weight thiol compounds—cysteamine, L-cysteine, and *N*-acetyl-L-cysteine—were subsequently tested for their potential antioxidative effects against hyaluronan degradation. It was shown that different final values of dynamic viscosity of hyaluronan solutions were dependent on the thiol structure and its initial concentration. An idea has been put forward that together with the reduction of the hyaluronan molecular weight, which is a consequence of fragmentation, the degradation products might contain associated or even cross-linked structures. In the case of *N*-acetyl-L-cysteine application, the carbonaceous residue evidenced by differential thermogravimetry was increased when compared to that of intact hyaluronan.

Keywords Hyaluronan · Rotational viscometry · Fourier-transform infrared spectroscopy · Non-isothermal methods

E. Hrabárová (✉)
Department of Carbohydrate Enzymology,
Institute of Chemistry, Slovak Academy of Sciences,
Dúbravská cesta 9, 84538 Bratislava, Slovak Republic
e-mail: eva.hrabarova@savba.sk

J. Rychlý · I. Janigová · K. Csomorová
Polymer Institute, Slovak Academy of Sciences,
84541 Bratislava, Slovak Republic

V. Sasinková
Department of Analytical Chemistry,
Institute of Chemistry, Slovak Academy of Sciences,
84538 Bratislava, Slovak Republic

K. Valachová · I. Juránek · L. Šoltés
Institute of Experimental Pharmacology and Toxicology,
Slovak Academy of Sciences, 84104 Bratislava,
Slovak Republic

Introduction

Though cellulose is the major component of biomass being extensively studied nowadays, not less is hyaluronan (HA) significant as the major component of extracellular matrix of vertebrates including humans.

Hyaluronan (Scheme 1) is a linear glycosaminoglycan built of the disaccharide repeating units comprising D-glucuronate linked via β-(1 $\rightarrow$ 3) glycosidic linkage to *N*-acetyl-D-glucosamine. These disaccharide structural units are linked via β-(1 $\rightarrow$ 4) glycosidic bonds.

HA is synthesized in the plasmatic membrane of various cells of vertebrates, and in tissues it functions in building-up of the extracellular matrices. Native HA macromolecules do not contain sulphate groups. HAs

Scheme 1 Hyaluronic acid polymer

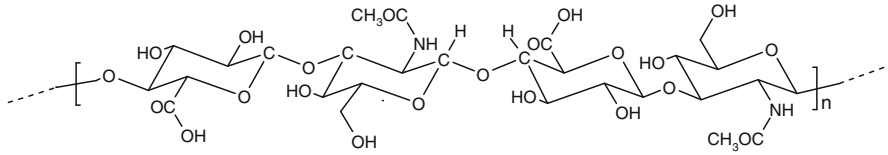

synthesized in vivo can reach the molecular weight values of up to 10^7 Da (Stern 2003).

High concentrations of HA in solution are very viscous (Kogan et al. 2007; Furth et al. 2008). The physiological level of HA in human synovial fluid (SF) is 2–4 mg/mL (Balazs et al. 1967). SF—a viscoelastic tissue—serves as a lubricant protecting cartilages against mechanical damage (Bastow et al. 2008). HA is characterized by an extraordinarily high rate of turnover. A 70 kg individual contains ≈15 g of this glycosaminoglycan. The one third of this amount turns over daily. The HA half-life in SF of healthy subjects is 12 h (Stern et al. 2007).

Under rheumatoid arthritis (RA) conditions the degradation of high-molecular-weight HA occurs due to the joint inflammation. Such a pathological situation is usually accompanied with the impairment and even the loss of the viscoelastic properties of SF. It was established that low-molecular-weight HA has different activities compared to the native high-molecular-weight biopolymer (Stern et al. 2007). While high-molecular-weight linear HAs are antiinflammatory with low angiogenic properties, the lower sized polymer fragments and branched or crosslinked HAs may have inflammatory, immunostimulatory, and highly angiogenic properties. HA fragments comprising 25–50 disaccharide units appear to function as endogenous danger signals (Stern 2004).

It is well-known that several endogenous thiols such as L-glutathione (GSH) act directly at scavenging of free radicals whose presence have been unambiguously evidenced at various diseases (RA and many others). GSH protects proteins against irreversible oxidation. The reaction between GSH and cysteine residues within a polypeptide chain is called *S*-glutathionylation (Hurd et al. 2005). Reversible formation of mixed disulphides prevents proteins in vivo from irreversible oxidations of their cysteine residues (Shenton and Grant 2003). *S*-Glutathionylated proteins may function as potential biomarkers of oxidative/nitrosative stress in some human diseases (Prakash et al. 2009). GSH has a special role not only as a biological antioxidant but also as a signalling molecule in the lung system regarding immunity and inflammation (Ghezzi 2011).

Recently, GSH has been tested for its significant antioxidative potential in the protection of high-molecular-weight HA against undesirable degradation (Hrabárová et al. 2009, 2012) induced by the *Weissberger*'s biogenic oxidative system (WBOS) (Weissberger and Luvalle 1944; Butt and Hallaway 1961). Prior to the application of non-isothermal methods, the Fourier-transform infrared (FT-IR) spectra of HAs recovered in a solid form after being treated via rotational viscometry revealed certain changes in comparison with the spectrum given for the intact HA, assuming thus a possible incorporation of thiol residue(s) into the HA macromolecule (Hrabárová et al. 2009).

In our study we investigated antioxidative effects of several cysteine-derived endogenous thiols (Scheme 2) such as cysteamine (CAM), L-cysteine (CYS), and *N*-acetyl-L-cysteine (NAC) using the method of rotational viscometry (RV). We also investigated potential structural changes of thiol-modified HAs after being thus processed in a solid form applying Fourier-transform infrared (FT-IR) spectroscopy, and non-isothermal methods such as chemiluminometry (CL), differential scanning calorimetry (DSC), and differential thermogravimetry (DTG).

Supposing that thiol compounds act as free radical scavengers and/or peroxide decomposers, our effort consisted in elucidation of their protective properties against the HA degradation induced by WBOS. A possible thiol incorporation into the HA macromolecule, recovered after degradation process in a solid form, was characterized via the methods such as CL, DSC and DTG. The CL method provides information about the relative efficiency of different antioxidants within a relatively large temperature interval. Moreover, when using an appropriate model of the HA degradation, the characterisation of the residual stability by the rate constant of the HA degradation may be more quantitative. As resulted from the DTG measurements, the possible extent of cross-linking may be deduced from the relative amount of carbonaceous residue that remains on the reaction pan.

Scheme 2 Cysteamine (*left*), L-cysteine (*middle*), and *N*-acetyl-L-cysteine (*right*)

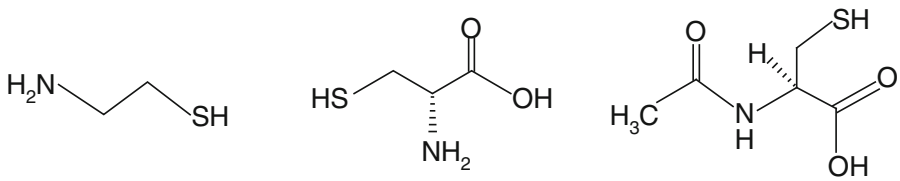

Finally, the DSC method which describes the extent of exothermic or endothermic process at higher temperatures may act as fingerprint of the structural changes in the HA macromolecules during their degradative fragmentation.

Experimental

Materials

High-molecular-weight HA (P9710-2A; $M_w = 808.7$ kDa; $M_w/M_n = 1.63$) was kindly donated from Lifecore Biomedical Inc., Chaska, MN, USA. CAM, CYS, and NAC—all of analytical purity grade were purchased from Sigma–Aldrich Chemie GmbH, Steinheim, Germany.

Methods

Rotational viscometry

The HA sample (2.5 mg/mL) was dissolved in 0.15 M aqueous NaCl solution for 24 h in the dark. The reagents were gradually added to the HA solution at the beginning of the reaction having final concentrations in the reaction system: 1.0 μM $CuCl_2$, 100 μM thiol compound, and 100 μM ascorbate. The changes of dynamic viscosity of the final reaction mixture (8.0 mL) were on-line monitored for the period of 5 h via rotational viscometry at 25 °C (Hrabárová et al. 2009). Applying the solvent-exchange method for polymer recovery in a solid form, the reaction product was subsequently precipitated pouring the aqueous solution into 20 mL of 96 % ethanol under extensive stirring, and kept at +4 °C overnight. The next day, the precipitate was thoroughly washed out with ethanol, acetone, and dried in air. The yields of the recovered polymers ranged between 67 and 92 % of the initial HA amount. The dried polymeric products were obtained in the form of amorphous consistence. Such thiol-modified HAs as particulates were further used to characterize their potential structural changes due to degradation.

Fourier-transform infrared spectroscopy

FT-IR spectra were measured with Nicolet 6700 (Thermo Fisher Scientific, USA) spectrometer equipped with DTGS detector and Omnic 8.0 software. The spectra were collected in the middle region from 4,000 to 400 cm^{-1} at a resolution of 4 cm^{-1}, the number of scans was 128. Diamond Smart Orbit ATR accessory was applied for measurement in solid state.

Differential scanning calorimetry

DSC measurements were performed using a Mettler-Toledo DSC 821^e differential scanning calorimeter. Indium was used for calibration of temperature and heat of fusion. Glass transition temperature (T_g) and thermal stability of the samples were evaluated from the second heating of samples from room temperature up to 550 °C (10 °C/min) in a nitrogen atmosphere (50 mL/min). The first heating (from room temperature up to 170 °C) was used for water removal. Thermooxidative degradation was investigated in a temperature range from room temperature up to 550 °C (10 °C/min) in an oxygen flow (50 mL/min). At least three parallel runs were performed for each sample.

Differential thermogravimetry

DTG measurements were performed using a Mettler-Toledo TGA/SDTA 851^e instrument in a nitrogen or oxygen flow (30 mL/min) using a heating rate of 2.5 °C/min in a temperature range from room temperature up to 550 °C. Indium and aluminium were used for temperature calibration.

Chemiluminometry

CL measurements were performed with a photon-counting instrument Lumipol 3 manufactured at the

Polymer Institute of the Slovak Academy of Sciences. The sample was placed on an aluminium pan in the sample compartment. The gas flow (pure oxygen or nitrogen) through the sample cell was 3.0 L/h. The temperature in the sample compartment of the apparatus was raised from 40 up to 250 °C with the rate of 2.5 °C/min. The signal of the photocathode was recorded at 10 s data collection interval.

Evaluation of non-isothermal chemiluminescence records

The CL signal intensity I depends on the rate of the oxidation process w according to the following relationship

$$I = \Phi w$$

Proportionality coefficient Φ is not constant when switching from one material to another; it depends on the geometry of the experiment, on the presence of quenchers of excited states, as well as on several other factors, which become revealed only after a detailed study of the respective system. The rate of oxidation, however, is a real variable that depends on the mechanism of the oxidation (degradation) process.

The kinetic model that was developed by Ekenstam (1936) and Emsley et al. (1997) for the degradation of cellulose is quite simple. Nevertheless, it may quantify the non-isothermal process which is a necessary prerequisite of any extrapolation or comparison of the effect of various additives. The degree of polymerisation (DP) is here understood as the ratio of concentration of monomer units (N) and polymer molecules (i) according to

$$DP = \frac{N}{i} \tag{1}$$

Due to degradation, the concentration of fragmented polymer molecules increases with time. Provided that the process takes place statistically, the kinetics of the concentration of macromolecules increase (for the case of degradation) and may be described by the following equation:

$$\frac{di}{dt} = mki^n \tag{2}$$

where n stands for the order of main chain scissions while $m = 1$ for the case of degradation (number of molecules increases). The most frequent reaction orders encountered in the literature are $n = 0$ or $n = 1$.

For the former case of $n = 0$ and $m = 1$

$$\frac{di}{dt} = k \text{ and } i = i_0 + kt \tag{3}$$

where i_0 is the initial concentration of macromolecules in the system. Here, the number of fragmented macromolecules increases linearly with the time of degradation. For DP, we then have:

$$DP = \frac{N}{i_0 + kt} \tag{4}$$

or

$$DP = \frac{DP_0}{1 + \frac{k}{i_0}t}$$

where $DP_0 = \frac{N}{i_0}$.

To develop an interpretation of non-isothermal CL runs, one needs to go back to the possible reactions leading to the light emission. CL generally expresses the rate of sample oxidation, where the intensity depends on a set of parameters such as the geometry of the sample, temperature, oxygen concentration, concentration of potential emitters, e.g., carbonyl groups in the sample, morphology and water content, etc. In the first approximation, it can be assumed that—similarly to isothermal conditions—the CL intensity I is proportional to the rate of hydroperoxide decomposition. At the same time, it may be assumed that the latter reflects the changes of the polymerisation degree.

$$I = \mu\left[-\frac{d[POOH]}{dt}\right] = \alpha\left[-\frac{dDP}{dt}\right] \tag{5}$$

where μ and α are the proportionality constants.

According to Eq. (4), $-\frac{dDP}{dt} = \frac{k}{i_0 DP_0} DP^2$ and for non-isothermal conditions:

$$-\frac{dDP}{dT}\frac{dT}{dt} = \frac{A\exp(-E/RT)}{i_0 DP_0} DP^2 \tag{6}$$

Here, T is the absolute temperature, A and E are the pre-exponential factor and the activation energy, respectively, and $\frac{dT}{dt} = \beta$ is the linear heating rate of the sample.

After integration of Eq. (6) and substitution into Eq. (5), we finally obtain, under non-isothermal conditions

$$I = \alpha \frac{A \exp(-E/RT)}{i_0} \frac{DP_0}{\left[1 + \frac{A}{\beta i_0} \int_{T_{room}}^{T} \exp(-E/RT) dT\right]^2} \quad (7)$$

It is noteworthy that while the process of the chain scission is of the zeroth order, the CL runs formally correspond to the second order scheme. For complex non-isothermal curves, it is preferable to use the sum of several independent processes, each of which has its proper *Arrhenius* dependence of the rate constant. In a case, e.g. two processes, the resulting equation suitable for fitting of non-isothermal data is the following:

$$I = \sum_{i=1}^{2} \frac{P_i \exp(-E_i/RT)}{\left[1 + \frac{A_i}{\beta i_0} \int_{T_{room}}^{T} \exp(-E_i/RT) dT\right]^2} \quad (8)$$

Here, P_i is the proportionality constant including the corresponding terms from Eq. (7), and A_i and E_i are, respectively the pre-exponential factor and the activation energy of component *i* of the initiation reaction. The latter values are used for calculation of the average rate constant of oxidation at a given temperature.

The average rate constant k_{av} for 2 components of initiation ($i = 2$), leading to the light emission, is defined as:

$$k_{av} = \frac{P_1}{P_1 + P_2} \frac{k_1}{i_0} + \frac{P_2}{P_1 + P_2} \frac{k_2}{i_0} \quad (9)$$

where k_1/i_0 and k_2/i_0 are rate constants at a given temperature of the respective initiating process. They have the unit of the first order reaction (s^{-1}). In practical computation procedures, one determines the corresponding parameters for any of the initiating events by non-linear regression analysis taking into account the experimental runs normalized to one at the maximum temperature of the experiment, i.e., 250 °C.

Results and discussion

Rotational viscometry

WBOS, contrary to the system proposed by Udenfriend (Udenfriend et al. 1954; Burkitt and Gilbert 1990), is a proper generator of hydrogen peroxide which is decomposed by the action of Cu(II)/Cu(I) ion system and thus of hydroxyl radicals. As evidenced in Fig. 1 (black line), the action of the WBOS on high-molecular-weight HA macromolecules resulted in a gradual decrease of the value of solution dynamic viscosity (η) from 9.93 to 6.53 mPa·s at the 5th h. In accord to the relationship η versus M_w, M_w determined for the HA polymer sample recovered after a 5-h viscometric treatment equalled to approx. 420 kDa. This value was taken from a calibration curve η versus M_w obtained for the HAs with exactly defined molecular characteristics (Valachová et al. in press). When the WBOS system is not applied, the viscosity of intact HA sample having starting value of $M_w = 808.7$ kDa does not practically change after 5 h when processed via the RV method. Such a system usually exhibits a well-known phenomenon of rheopexy (Šoltés et al. 2005).

As resulted from a free-radical chain reaction given for the HA macromolecules initiated by $^{\bullet}OH$ radicals (Ghezzi 2011), the action of the added thiols—CAM, CYS, and NAC—reduced the extension of the polymer degradation in a different manner. Thus we could speak about thiol antioxidative action proved by scavenging of $^{\bullet}OH$ radicals.

$$R{-}SH + {}^{\bullet}OH \rightarrow R{-}S^{\bullet} + H_2O \quad (10)$$

Here R–SH by reaction 10 competes efficiently with HA (HA–C–H; reaction 11) and the harmful effect of

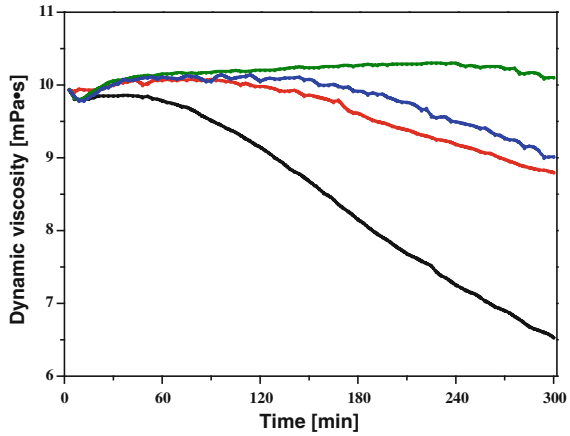

Fig. 1 Antioxidative effects of endogenous thiols against high-molecular-weight hyaluronan (P9710-2A; 2.5 mg/mL) degradation induced by the action of the *Weissberger*'s oxidative system. Reference probe sample: 100 µM ascorbate *plus* 1.0 µM $CuCl_2$ (*black*). Concentration of cysteamine (*green*), L-cysteine (*red*), and *N*-acetyl-L-cysteine (*blue*), added into the reaction system before the onset of the reaction, in µM: 100. (Color figure online)

hydroxyl radicals against the HA macromolecules is reduced

$$HA{-}C{-}H + {}^{\bullet}OH \rightarrow HA{-}C^{\bullet} + H_2O \quad (11)$$

As seen in Fig. 1, the order of viscosity pronounced decrease is as follows: CYS<NAC<CAM. A reaction between the thiyl radical and the *C*-type HA macroradical (HA–C$^{\bullet}$) during initial phase of the HA degradation may come into consideration as well (reaction 12).

$$HA{-}C^{\bullet} + R{-}S^{\bullet} \rightarrow HA{-}C{-}S{-}R \quad (12)$$

This possible incorporation of a sulphur atom into the HA structure, which we could name "thiylation", is documented recently using GSH in the function of a radical scavenger against the HA degradation by WBOS (Hrabárová et al. 2009). The same process could occur also in the case of CAM, CYS, NAC. To prove or disprove this statement, the FT-IR method can be the primary choice.

Based on the measurements of the dynamic viscosity changes (Fig. 1), it is evident that only slight changes may be observed in the case of CAM while NAC and CYS showed significantly lower protective effects against free-radical degradation of HA macromolecules. One should be aware that the results provided by the RV method may not only indicate the drop of antioxidative properties of the thiol additive but they may also indicate a potential occurrence of branching or even cross-linking during the HA modification. Then the resulting pattern of the viscosity changes could be the superposition of both processes.

A novel disulphidic HA-cysteine ethyl ester conjugate via cross-linking process was prepared which significantly reduced the rate of the polymer degradation (Kafedjiiski et al. 2007). A possible way of cross-linking may occur between HA and NAC forming HA-*N*-acetyl-L-cysteine conjugate. We may therefore name it "thiylated" HA. A question has been arisen if there is a real possibility that synovial HA could be stabilized against the biodegradation via disulphide bond-created cross-linked formation. However, under favourable conditions, the mechanism of such a process should involve the formation of amidic bond by condensation reaction from the HA carboxyls and amino group of thiol. The subsequent formation of disulphides via recombination reaction of thiyl radicals (termination reaction 13) should be followed by mixed formations of the HA disulphides with a thiol moiety (reaction 14), and finally by the formation of the HA disulphides (reaction 15):

$$R{-}S^{\bullet} + R{-}S^{\bullet} \rightarrow R{-}S{-}S{-}R \quad (13)$$

$$HA{-}C^{\bullet} + R{-}S{-}S{-}R \rightarrow R^{\bullet} + HA{-}C{-}S{-}S{-}R \quad (14)$$

$$HA{-}C^{\bullet} + HA{-}C{-}S{-}S{-}R \rightarrow R^{\bullet} + HA{-}C{-}S{-}S{-}C{-}HA \quad (15)$$

Fourier-transform infrared spectroscopy

As shown from detailed analyses of the FT-IR spectral records obtained for thiol-modified HA samples and intact HA (Figs. 2, 3, and 4), certain changes were revealed in their spectral bands differing from that of the intact HA sample. The wavenumber region at 1,200–900 cm^{-1} is characteristic for vibrations of carbohydrates. Characteristic absorption bands are typical for each polysaccharide taking into account the overlap of absorption bands of the stretching ν(C–O), ν(C–C) and bending δ(C$_1$–OH) vibrational modes of corresponding monosaccharide units, and of the glycosidic bond ν(C–O–C) at about 1,150 cm^{-1} (Gilli et al. 1994; Kačuráková et al. 2000). At 730–570 cm^{-1} is a region which includes the C–S bond vibrations (Günzler and Gremlich 2002). These vibrations usually have weak intensities and, in the case of thiol-modified HA samples they are hardly to be noticed.

Physical properties of polysaccharides due to the hydrogen bond formation applying various drying methods are usually changed. This phenomenon can be studied by FT-IR for the –OH bond stretching regions. Besides free –OH groups, there are hydrogen bonds present as both inter- and intramolecular in polymer. Their ratio and interactions as a result of polymer modifications are therefore changed (Hromádková et al. 2003). As a consequence of the changed inter- and intramolecular hydrogen bond formation in the thiol-modified HA, the main maximum peak for the monosaccharide unit of polymer was shifted from 1,036 cm^{-1} as given for the intact HA to the lower values of wavenumber that was in the case of the thiol-modified HAs as follows: CYS 1,032 cm^{-1}, CAM 1,030 cm^{-1}, and NAC 1,026 cm^{-1} (Fig. 2). This was accompanied also with the increase of the half-width of the band. Among all the thiols, NAC exhibited the greatest influence on the shift of the main maximum peak that was 10 cm^{-1}. As resulted from the changed

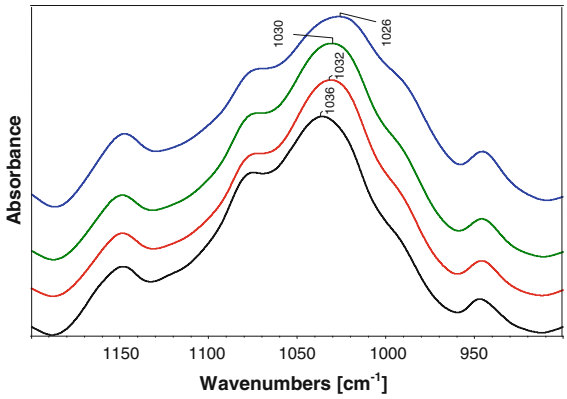

Fig. 2 Fourier-transform infrared spectral records of the main maximum peak for the monosaccharide unit of hyaluronan that was shifted to the lower values of wavenumber as given for the thiol-modified hyaluronans: *N*-acetyl-L-cysteine-modified hyaluronan (*blue*); cysteamine-modified hyaluronan (*green*); L-cysteine-modified hyaluronan (*red*); intact hyaluronan—P9710-2A (*black*). (Color figure online)

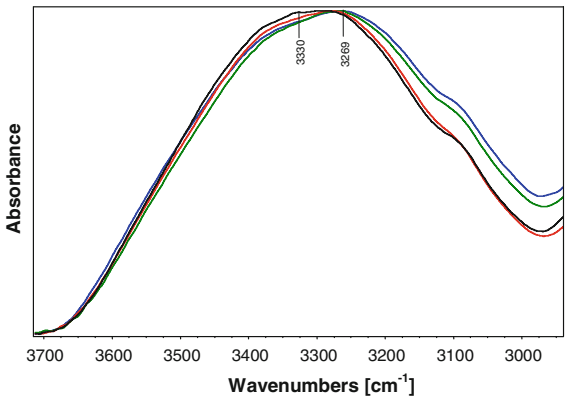

Fig. 3 Fourier-transform infrared spectral records in the region of stretching vibrations of the –OH bond for the thiol-modified hyaluronans: *N*-acetyl-L-cysteine-modified hyaluronan (*blue*); cysteamine-modified hyaluronan (*green*); L-cysteine-modified hyaluronan (*red*); intact hyaluronan—P9710-2A (*black*). (Color figure online)

ratio of inter- and intramolecular bond formation in polymer, band maximum position for stretching vibration ν(OH) bond was as well shifted from 3,330 cm^{-1} as given for the intact HA (Günzler and Gremlich 2002) to the lower frequencies 3,269 cm^{-1} as given for thiol-modified HAs accompanied with the broadening of the half-width of the band (Fig. 3).

It is known that FT-IR spectra of the stretching vibrations ν(C–H) bonds (–CH_3, –CH_2, –CH groups) have their absorption peaks in the wavenumber region 3,000–2,800 cm^{-1} (Günzler and Gremlich 2002). In

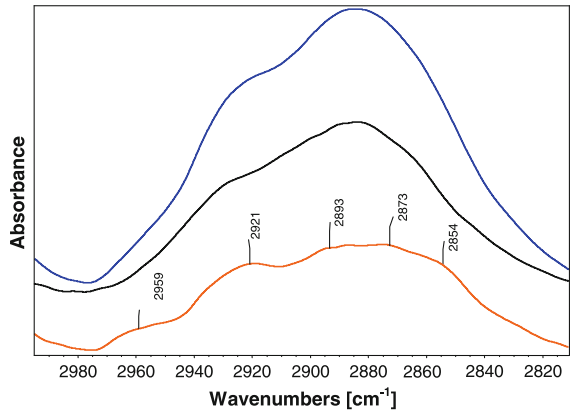

Fig. 4 Fourier-transform infrared differential spectral records in the region of stretching vibrations for –CH bonds for *N*-acetyl-L-cysteine-modified hyaluronan (*blue*) and intact hyaluronan—P9710-2A (*black*). The structural changes are indicated by five different values of wavenumbers as given by the subtraction spectrum between *N*-acetyl-L-cysteine-modified hyaluronan and intact hyaluronan (*orange*). (Color figure online)

this region we can observe a differential FT-IR spectrum obtained using a subtraction technique for the NAC-modified HA (Fig. 4). The increase of the C–H vibration intensities for individual groups was significant. Asymmetrical stretching vibration ν_{as}(C–H) bond and symmetrical stretching vibration ν_s(C–H) bond from the –CH_3 group was at 2,959 cm^{-1} and 2,873 cm^{-1}. The ν_{as}(C–H) bond was at 2,921 cm^{-1} and the ν_s(C–H) bond was at 2,854 cm^{-1} from the –CH_2 group. Stretching vibration ν(C–H) bond from the C–H group was at 2,893 cm^{-1}. The increase of the band intensities in the region of the C–H vibrations was evidenced from the differential FT-IR spectrum. Based on our results, we can thus assume the formation of a thiol-modified HA structure during viscometric processing.

Chemiluminometry

The CL method is routinely used as a suitable analysis tool on in vitro study of spontaneous oxidative aging e.g. cellulosic materials (Rychlý et al. 2004). The same method was successfully applied to investigate structural changes in the HA macromolecules after accelerated oxidative aging in vivo (Rychlý et al. 2006).

The large difference between the CL intensity and the DSC heat release in oxygen and in nitrogen indicates that the degradation was governed predominantly by the reactions of peroxyl radicals or

eventually by the decomposition of the hydroperoxides formed in the degradation process (reactions 16, 17, and 18).

$$HA-C^{\bullet} + O_2 \rightarrow HA-C-O-O^{\bullet} \quad (16)$$

$$HA-C-O-O^{\bullet} + HA-C-H \rightarrow HA-C-O-OH + HA-C^{\bullet} \quad (17)$$

$$HA-C-O-OH \rightarrow HA-C-O^{\bullet} + {}^{\bullet}OH \quad (18)$$

Decomposition of hydroperoxides with the formation of alkoxyl and hydroxyl radicals is responsible for the oxidative fragmentation of the HA macromolecules occurring as β-scission of the HA alkoxyl radicals.

In the case of chemiluminescence (Scheme 3), the most probable candidate reaction providing light emission is disproportionation of peroxyl radicals (Zlatkevich 1989; Billingham et al. 1991; Celina and George 1995; Matisová-Rychlá and Rychlý 1996; Kohler and Krohnke 1998; Setnescu et al. 1998; Rychlý et al. 2000; Blakey 2001; Gijsman and Verdun 2001; Rychlý et al. 2004). On the other hand, exotherms in the case of DSC (Scheme 4) are mainly due to the propagation reaction of peroxyl radicals (Rychlý et al. 2006).

By non-linear regression analysis of CL intensity versus temperature runs it was revealed that the rate of degradation was composed of several processes having different rates of initiation. We have thus determined the rate constants of the residual oxidative degradation of HA at respective temperature. Of particular importance is that the measurement has been done over the large temperature interval that enabled to perform evaluation of the rate constants of degradation which fits the temperature interval examined (40–250 °C). The average values of the rate constants that are linked with residual thermooxidative stability of HA for the temperatures 40, 100, 200 and 230 °C are given in Table 1 and their *Arrhenius* plots are shown in Fig. 5. Typically the rate constants of residual degradation at 40 °C are ordered as follows:

$$CAM < CYS < NAC < HA$$

which corresponds to the sequence of dynamical viscosity decrease after 5 h-modification of HA by WBOS during viscometric measurement. Though the order of the respective rate constants at higher temperatures changes differentiating the themooxidative effect of thiols at thermal oxidation, the above results indicate that the link between the RV and the CL measurements extrapolated to low temperatures is very realistic.

It is of interest that antioxidative properties of NAC were evidenced only at elevated temperatures (Table 1). NAC seems thus to have little effect on the HA fragmentation at lower temperatures (till 100 °C) observed. The position of the maximum of respective records in the oxygen measurements (Fig. 6) on the temperature scale from left to right is: intact HA<HA–CAM<HA–CYS<HA–NAC. The

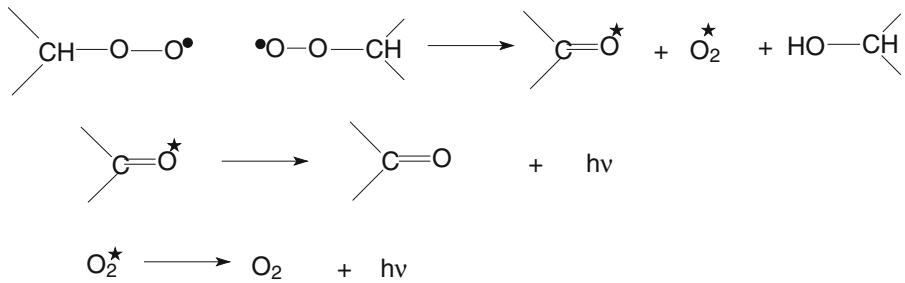

Scheme 3 Presumptive formation of carbonyls and oxygen emitting light via disproportionation reaction of peroxyl radicals tested via chemiluminometry. Asterisks denote the excited states of ketones (*triplet*) and oxygen (*singlet*), which are converted to the ground state with the emission of light

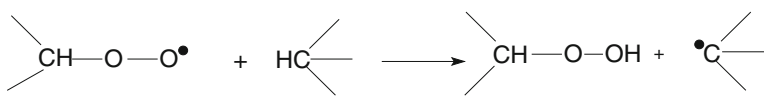

Scheme 4 Propagation reaction of peroxyl radicals forming hydroperoxides and alkyl radicals tested via differential scanning calorimetry

Table 1 The average rate constants k_{av} of oxidation determined from chemiluminescence measurements in oxygen according to the Eqs. (8) and (9) for the intact hyaluronan and that of modified with various thiols at the temperatures: 40, 100, 200, or 230 °C, respectively

Sample	k_{40} [s^{-1}]	k_{100} [s^{-1}]	k_{200} [s^{-1}]	k_{230} [s^{-1}]
Intact hyaluronan	$1.1e^{-9}$	$1.6e^{-7}$	$6.3e^{-4}$	$2.2e^{-2}$
L-Cysteine-modified hyaluronan	$7.0e^{-10}$	$3.2e^{-7}$	$4.6e^{-4}$	$4.9e^{-3}$
N-Acetyl-L-cysteine-modified hyaluronan	$8.0e^{-9}$	$1.2e^{-6}$	$5.0e^{-4}$	$4.4e^{-3}$
Cysteamine-modified hyaluronan	$1.2e^{-10}$	$7.5e^{-8}$	$2.8e^{-4}$	$1.16e^{-2}$

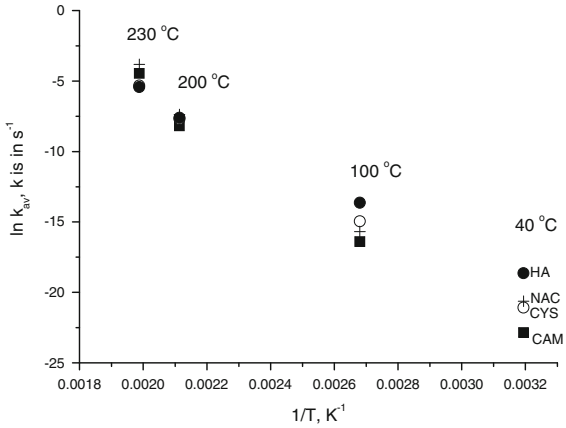

Fig. 5 The *Arrhenius* plots of the average rate constants k_{av} of residual oxidation determined from chemiluminescence measurements in oxygen according to the Eqs. (8) and (9) for the intact hyaluronan and that of modified with various thiols at the temperatures: 40, 100, 200, or 230 °C, respectively

order of the maximum of respective records remained the same in the nitrogen measurements (Fig. 7). Supposing that all the not reacted thiol traces were removed from the system by thorough washing out, this shift may be explained by binding of the thiol moiety to the HA macromolecule, and keeping in this way the antioxidative properties. Particular situation is represented by the CL record of NAC-modified HA (Figs. 6 and 7) that exhibited the lowest value of the maximum CL intensity (more than tenfold) when compared to the other thiol-modified HAs. This may be the indication that NAC is bound to the HA macromolecule to a significantly higher extent than the other thiols are. CL records for the thiol-modified

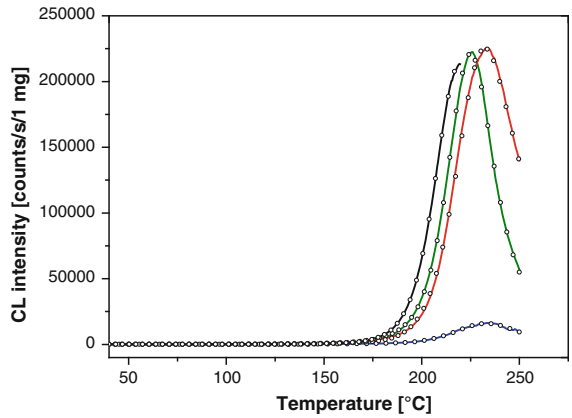

Fig. 6 Chemiluminescence records in oxygen for hyaluronan (*black*) and for the thiol-modified hyaluronans: L-cysteine (*red*), *N*-acetyl-L-cysteine (*blue*), and cysteamine (*green*). The rate of heating: 2.5 °C/min. The points denote theoretical runs of chemiluminescence intensity versus temperature obtained by fitting of experiments by the Eq. (8). (Color figure online)

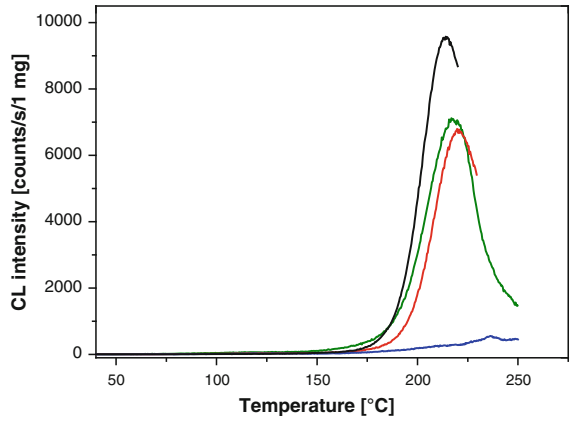

Fig. 7 Chemiluminescence records in nitrogen for hyaluronan (*black*) and for the thiol-modified hyaluronans: L-cysteine (*red*), *N*-acetyl-L-cysteine (*blue*), and cysteamine (*green*). The rate of heating: 2.5 °C/min. (Color figure online)

HAs were much more intense (more than 30 times) in oxygen (Fig. 6) than in nitrogen (Fig. 7).

Differential scanning calorimetry

The DSC records for HA (Fig. 8) provided the two exotherms A and B situated at 232 and 257 °C in oxygen, and at 239 and 258 °C in nitrogen. In oxygen the additional exotherm C appeared with a maximum at 341 °C which obviously belongs to the oxidation of the char residue formed from the cross-linked HA.

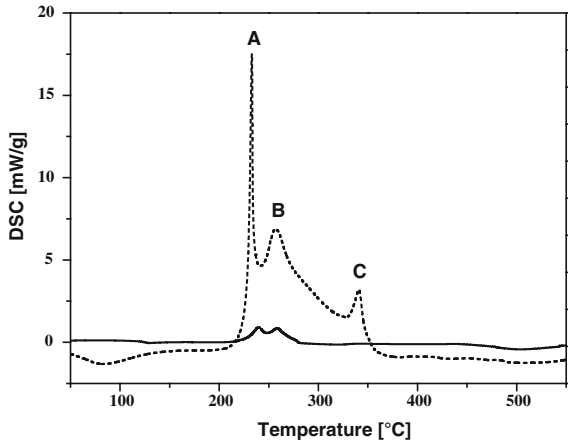

Fig. 8 Differential scanning calorimetry records for the intact hyaluronan in oxygen (*dotted line*) and in nitrogen (*full line*). The rate of heating: 10 °C/min

One should be aware of the fact that exotherms obtained by the DSC records are usually the result of oxidation.

The same position of the DSC exotherms A and B in nitrogen was found also for CAM- and CYS-modified HAs (Fig. 9). At the same time, the two exotherms indicate that in the recovered polymers two types of reaction sites exist differing by their reactivity towards subsequent transformation. The observation that the exotherm B for the NAC-modified HA disappeared and/or was replaced by a not very distinct shoulder is also worth of noticing. The absence of this

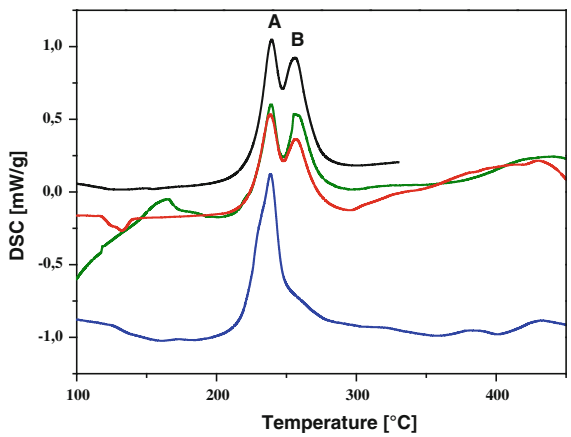

Fig. 9 Differential scanning calorimetry records (section from 100 to 450 °C) in nitrogen for intact hyaluronan (*black*) and for the thiol-modified hyaluronans: L-cysteine (*red*), *N*-acetyl-L-cysteine (*blue*), and cysteamine (*green*). The rate of heating: 10 °C/min. (Color figure online)

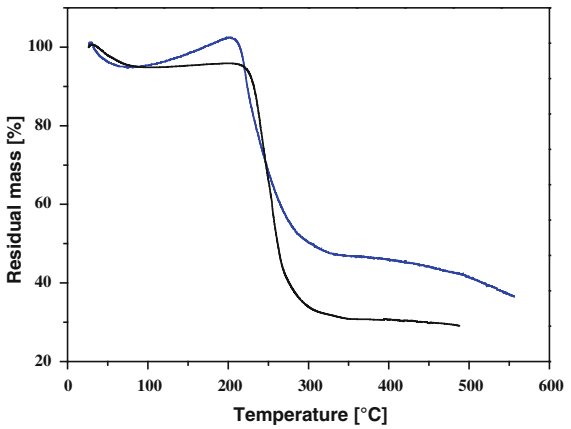

Fig. 10 Differential thermogravimetry records in oxygen for the *N*-acetyl-L-cysteine-modified hyaluronan (*blue*)—the rate of heating 2.5 °C/min, and for intact hyaluronan (*black*)—the rate of heating 10 °C/min. (Color figure online)

exotherm might be brought about by the extensive fragmentation of the higher-molecular-weight fraction of the HA polymer which is documented by the RV method (Fig. 1): the decrease of viscosity in the case of NAC-modified HA preceded that of CAM- and CYS-modified HAs.

Differential thermogravimetry

As resulted from the DTG records in oxygen (Fig. 10), relatively large residue remained in the pan after the sample heating to 500 °C. A particularly distinct situation was in the case of the NAC-modified HA where the increase of the mass in the temperature interval of approx. 100–200 °C occurred that was probably due to the direct reaction of the thiol additive with the HA macromolecule forming relatively stable conjugates/associates or even cross-linked structures.

Conclusions

On the basis of our results, we may conclude that:

1. Intact HA solutions were modified by the action of WBOS at the presence of the thiol compounds (CAM, CYS, and NAC) via the RV method. As a result of the degradation process, HAs were fragmented to a various final dynamic viscosity dependently on thiol applied. The results given by the FT-IR, CL, DSC, and DTG methods support

the assumption that incorporation of a thiol moiety into the HA macromolecule forming associated or even cross-linked structures could be significant.

2. While decrease of dynamic viscosity was the result of the HA fragmentation during degradation, eventually combined with cross-linking of the HA macromolecules acting both in the opposite directions, the DSC signal in nitrogen revealed the disappearance of the second exotherm for the NAC-modified HA which indicates the additional fragmentation of higher-molecular-weight fraction. In the case of the NAC application, the carbonaceous residue evidenced by the DTG method was increased when compared to that of the intact HA.
3. The CL method appears to be an efficient tool for delimitation of the residual stability and the antioxidative efficiency of thiol-modified HAs along a relatively large temperature scale. At lower temperatures the corresponding link with the residual viscosity of HA and the rate constants of degradation may be clearly seen. Binding thiol moieties to the HA macromolecules during degradation was deduced from the shift of non-isothermal chemiluminescence records to higher temperatures when compared to that of the intact HA.
4. Intensities of both the CL and DSC signals are considerably stronger in oxygen than in nitrogen which may be taken as the proof of the participation of peroxyl radicals in the HA degradation.

Acknowledgments The work was supported by the VEGA grant project Nos.: 2/0083/09, 1/0529/09, 2/0056/10, 1/0145/10, 2/0011/11 and 2/0147/12 of the *Slovak Academy of Sciences*. This contribution is the result of the project implementations: ITMS26220120054 and ITMS26240220040 supported by the Research & Development Operational Programme funded by the ERDF.

References

Balazs EA, Watson D, Duff IF, Roseman S (1967) Hyaluronic acid in synovial fluid. I. Molecular parameters of hyaluronic acid in normal and arthritis human fluids. Arthritis Rheum 10:357–376

Bastow ER, Byers S, Golub SB, Clarkin CE, Pitsillides AA, Fosang AJ (2008) Hyaluronan synthesis and degradation in cartilage and bone. Cell Mol Life Sci 65:395–413

Billingham NC, Then ETH, Gijsman P (1991) Chemiluminescence from peroxides in polypropylene. Part I: relation of luminescence to peroxide content. Polym Degrad Stab 34:263–277

Blakey I (2001) Aspects of the oxidative degradation of polypropylene. Dissertation, Queensland University of Technology, Brisbane

Burkitt MJ, Gilbert BC (1990) Model studies of the iron-catalysed Haber–Weiss cycle and the ascorbate-driven Fenton reaction. Free Radic Res Commun 10:265–280

Butt VS, Hallaway M (1961) The catalysis of ascorbate oxidation by ionic copper and its complexes. Arch Biochem Biophys 92:24–32

Celina M, George GA (1995) Heterogeneous and homogeneous kinetic analyses of the thermal oxidation of polypropylene. Polym Degrad Stab 50:89–99

Ekenstam A (1936) Behaviour of cellulose in solutions of mineral acids. Part II: a kinetic study of cellulose degradation in acid solutions. Ber Dtsch Chem Ges 69:553–559

Emsley AM, Heywood RJ, Ali CMM, Eley CM (1997) On the kinetics of degradation of cellulose. Cellulose 4:1–5

Furth G, Knierim R, Buss V, Mayer C (2008) Binding of bivalent cations by hyaluronate in aqueous solution. Int J Biol Macromol 42:33–40

Ghezzi P (2011) Role of glutathione in immunity and inflammation in the lung. Int J Gen Med 4:105–113

Gijsman P, Verdun F (2001) The influence of polymer type, stabilizers, and sample geometry on the relationship between chemiluminescence and oxygen uptake. Polym Degrad Stab 74:533–542

Gilli R, Kačuráková M, Mathlouthi M, Navarini L, Paoletti S (1994) FTIR studies of sodium hyaluronate and its oligomers in the amorphous solid phase and in aqueous solution. Carbohydr Res 263:315–326

Günzler H, Gremlich H-U (2002) IR spectroscopy. Wiley, Weinheim

Hrabárová E, Valachová K, Rychlý J, Rapta P, Sasinková V, Malíková M, Šoltés L (2009) High-molar-mass hyaluronan degradation by Weissberger's system: pro- and anti-oxidative effects of some thiol compounds. Polym Degrad Stab 94:1867–1875

Hrabárová E, Valachová K, Juránek I, Šoltés L (2012) Free-radical degradation of high-molar-mass hyaluronan induced by ascorbate plus cupric ions: evaluation of antioxidative effect of cysteine-derived compounds. Chem Biodiv 9:309–317

Hromádková Z, Ebringerová A, Sasinková V, Šandula J, Hříbalová V, Omelková J (2003) Influence of the drying method on the physical properties and immunomodulatory activity of the particulate (1 → 3)-β-D-glucan from *Saccharomyces cerevisiae*. Carbohydr Polym 51:9–15

Hurd TR, Costa NJ, Dahm CC, Beer SM, Brown SE, Filipovska A, Murphy MP (2005) Glutathionylation of mitochondrial proteins. Antioxid Redox Signal 7:999–1010

Kačuráková M, Capek P, Sasinková V, Wellner N, Ebringerová A (2000) FT-IR study of plant cell wall model compounds: pectic polysaccharides and hemicelluloses. Carbohydr Polym 43:195–203

Kafedjiiski K, Jetti RKR, Föger F, Hoyer H, Werle M, Hoffer M, Bernkop-Schnürch A (2007) Synthesis and in vitro

evaluation of thiolated hyaluronic acid for mucoadhesive drug delivery. Int J Pharm 343:48–58

Kogan G, Šoltés L, Stern R, Gemeiner P (2007) Hyaluronic acid: a natural biopolymer with a broad range of biomedical and industrial applications. Biotechnol Lett 29:17–25

Kohler DR, Krohnke C (1998) Chemiluminescence as an industrial test method for antioxidant effectiveness in polyolefins. 1. Fundamental considerations. Polym Degrad Stab 68:385–393

Matisová-Rychlá L, Rychlý J (1996) Inherent relations of chemiluminescence and thermooxidation of polymers. In: Clough RL, Billingham NC, Gillen KT (eds) Polymers durability, degradation and stabilisation. Advances in chemistry series 249, Am Chem Soc, Washington, pp 175–193

Prakash M, Shetty MS, Tilak P, Anwar N (2009) Total thiols: biomedical importance and their alteration in various disorders. Online J Health Allied Scs 8:1–9

Rychlý J, Matisová-Rychlá L, Jurčák D (2000) Chemiluminescence from oxidized polypropylene during temperature cycling. Polym Degrad Stab 68:239–246

Rychlý J, Matisová-Rychlá L, Lazár M, Slovák K, Strlič M, Kočar D, Kolar J (2004) Thermal oxidation of cellulose investigated by chemiluminescence. The effect of water at temperatures above 100 °C. Carbohydr Polym 58:301–309

Rychlý J, Šoltés L, Stankovská M, Janigová I, Csomorová K, Sasinková V, Kogan G, Gemeiner P (2006) Unexplored capabilities of chemiluminescence and thermoanalytical methods in characterization of intact and degraded hyaluronans. Polym Degrad Stab 91:3174–3184

Setnescu R, Jipa S, Osawa Z (1998) Chemiluminescence study on the oxidation of several polyolefins. I. Thermal-induced degradation of additive-free polyolefins. Polym Degrad Stab 60:377–383

Shenton D, Grant CM (2003) Protein S-thiolation targets glycolysis and protein synthesis in response to oxidative stress in the yeast *Saccharomyces cerevisiae*. Biochem J 374: 513–519

Šoltés L, Stankovská M, Kogan G, Gemeiner P, Stern R (2005) Contribution of oxidative-reductive reactions to high-molecular-weight hyaluronan catabolism. Chem Biodivers 2:1242–1245

Stern R (2003) Devising a pathway for hyaluronan catabolism: are we there yet? Glycobiology 13:105R–115R

Stern R (2004) Hyaluronan catabolism: a new metabolic pathway. Eur J Cell Biol 83:317–325

Stern R, Kogan G, Jedrzejas MJ, Šoltés L (2007) The many ways to cleave hyaluronan. Biotechnol Adv 25:537–557

Udenfriend S, Clark CT, Axelrod J, Brodie BB (1954) Ascorbic acid in aromatic hydroxylation. I. A model system for aromatic hydroxylation. J Biol Chem 208:731–739

Valachová K, Baňasová M, Machová Ľ, Juránek I, Bezek Š, Šoltés L (in press) Testing various hexahydropyridoindoles to act as antioxidants. In: New perspectives in chemistry and biochemistry. Nova Science Publishers, New York

Weissberger A, Luvalle JE (1944) Oxidation processes. XVII. The autooxidation of ascorbic acid in the presence of copper. J Am Chem Soc 66:700–705

Zlatkevich L (ed) (1989) Chemiluminescence in evaluating thermal oxidative stability of polymers. In: Luminescence technique in solid state polymer research. Marcel Dekker Publishing House, New York